药学学报 Acta Pharmaceutica Sinica 2011, 46 (8): 962−967

Tissue distribution of *s*-oleylpropanolamide in rats detected by liquid chromatography with tandem mass spectrometry

ZHENG Cheng-wei, JIN Xin*, SHEN Yan-hui, MA Ang, LU Wei

(*Department of Pharmacy, Medical College of Xiamen University, Xiamen 361005, China*)

Abstract: This paper is to report the development of a rapid and sensitive method for the determination of *s*-oleylpropanolamide (OPA) in various tissues of rat (brain, heart, lung, liver, spleen, small intestine, kidney, adipose tissue and muscle), and to assess the applicability of the assay to tissue distribution. OPA was extracted by liquid-liquid extraction method with undecylenoylethanolamide as an internal standard. The concentrations of OPA were determined by LC-MS/MS after a single intragastric dose of 50 mg·kg^{-1} at 4 time points (5 rats per group). With multiple reactions monitoring mode (MRM) the limit of quantification (LLOQ) was determined at 1 μg·L^{-1}. The calibration curve was linear from 1 to 2×10^4 μg·L^{-1} ($r \geqslant 0.999\ 0$) for tissue homogenates. Validation parameters such as accuracy, precision and recovery were found to be within the acceptance criteria of the assay validation guidelines. The highest concentration was found in small intestine (the highest time point is 15 min) and heart (the highest time point is 90 min). The assay is rapid, sensitive and applicable to studying tissue distribution of OPA in rats.

Key words: *s*-oleylpropanolamide; LC-MS/MS; tissue distribution

CLC number: R963 **Document code**: A **Article ID**: 0513-4870 (2011) 08-0962-06

液相色谱−质谱联用法对大鼠体内 *s*-油酰丙醇胺的组织分布研究

郑城微, 金 鑫*, 沈燕慧, 马 昂, 卢 伟

(厦门大学医学院药学系, 福建 厦门 361005)

摘要: 建立大鼠不同组织 (脑、心、肺、肝、脾、小肠、肾、脂肪和肌肉) 中 *s*-油酰丙醇胺含量的测定方法, 并研究 *s*-油酰丙醇胺在大鼠体内的组织分布情况。*s*-油酰丙醇胺提取采用液−液萃取, 以 10-十一烯酰乙醇胺为内标。SD 雄性大鼠灌胃给予 *s*-油酰丙醇胺 (50 mg·kg^{-1}) 后, 于 4 个时间点 (各时间点 5 只大鼠) 处死大鼠后, 取相应组织匀浆处理, 通过 LC-MS/MS 法测定其各脏器或组织中浓度。通过多反应检测模式测得定量下限 1 μg·L^{-1}, 各组织匀浆中 *s*-油酰丙醇胺在 1～2×10^4 μg·L^{-1} 内线性良好 ($r \geqslant 0.999\ 0$), 方法经验证符合生物样品分析要求。灌胃给药后药物浓度最高的组织为小肠和心脏, 达峰时间分别为 15 和 90 min。该法操作简便、灵敏度高, 适用于 *s*-油酰丙醇胺在大鼠体内的组织分布研究。

关键词: *s*-油酰丙醇胺; LC-MS/MS; 组织分布

Peroxisome proliferator-activated receptor-alpha (PPARα) is activated by both naturally occurring fatty-acid amide, and synthetic ligands such as fibrates which are widely used in the treatment of dyslipidemia[1, 2]. Oleylethanolamide (OEA) is a naturally occurring lipid that binds with high affinity to PPARα with the functions of lowering body weight and hyperlipidemia in obese rats[3−5]. Report has been shown that OEA involved the enzymatic hydrolysis of this lipid amide to oleic acid and ethanolamine[6, 7]. Other natural ligands such

Received 2011-01-19.
Project supported by Strait (Xiamen) Technology Platform in Traditional Chinese Medicine (3502Z20100006); and by National Natural Science Foundation of China (30670512).
*Corresponding author Tel: 86-592-2188676,
E-mail: xinjin@xmu.edu.cn

as palmitoylethanolamide was proved to mediate the anti-inflammatory effects by engaging PPARα like its analog OEA[8]. *s*-Oleylpropanolamide (OPA) which is a synthetic analog of OEA, resists enzymatic hydrolysis and prevents the development of atherosclerotic lesion formation by activating PPARα[9]. Previous studies have showed that OPA obviously prevented hyperdyslipidemia and inflammation with an intragastric administration of OPA at 100 mg·kg^{-1} in mouse (these results have not been published). These results provided new insights of OPA into possible future therapeutic approaches to the treatment of atherosclerosis.

Methods used in quantification of endocannabinoids in previous studies were all quantified by isotope-dilution with LC-MS or GC-MS[10, 11] and no such method of OPA has been published for quantification or for observing tissue distribution in animal model.

Previous study in our laboratory in pharmacokinetics of OPA has shown a rapid absorption and elimination (not published yet). In present study, a simple and highly sensitive LC-MS/MS method was developed and validated to determine concentration levels of OPA in rat tissue homogenates. The newly developed method is applied in tissue distribution study following intragastric administration of OPA in rats.

Materials and methods

Chemicals OPA (purity 98%) was synthesized in our laboratory, its chemical structure was identified by comparing the spectral properties with reported data[12]. Undecylenoylethanolamide (purity ≥ 90%, internal standard) was also synthesized in our laboratory.

Animal Male Sprague-Dawley rats, weighing 200 − 220 g, were obtained from Slac laboratory, Shanghai, China [SCXX (Shanghai) 2007-0005]. The tissues or organs, including brain, heart, lung, liver, spleen, small intestine, kidney, adipose tissue and muscle, were rinsed with physiological saline solution, and stored at −80 ℃ until analysis.

LC conditions An HP 1200 HPLC system (Agilent Technologies, Santa Clara, CA, USA), equipped with a reversed phase ODS-2 Hypersil column (150 mm × 4.6 mm ID, 5 μm; Thermo Scientific) was used in the study for the chromatographic separation of OPA and the IS. Mobile phase A was pure water. Mobile phase B consisted of 100% methanol. Gradient elution was performed at a flow rate of 1 mL·min^{-1}. The initial composition of the gradient was 80% B. This was held for the first minute. At 1 min phase B increased to 100% B within 0.2 min where it was held for 4 min. At 5 min, gradient returned to initial conditions of 80% B to re-equilibrate the column. The total running time was 6.5 min. In this study, the sample volume was set at 10 μL.

MS conditions Mass spectrometric detection was performed with a Qtrap 3200 system (AB/MDS SCIEX Instruments, CA), equipped with an atmospheric pressure chemical ionization (APCI) source operating in positive-ion mode. Quantification was done by using the multiple reaction monitoring (MRM) transitions *m/z* 340.3→76.1 for OPA and 228.0→62.1 for the IS. Data acquisition and processing were performed with the analyst 1.4.1 software version (AB/MDS SCIEX Instruments, CA).

Standards and quality control (QC) samples Stock solution of OPA (1×10^6 μg·L^{-1}) and IS (1×10^5 μg·L^{-1}) were prepared by dissolving the compounds in methanol. A set of OPA standard solutions was obtained by a successive dilution of the stock solution with methanol. 10 μL aliquots of these standard solutions were spiked to 100 μL of blank rat different tissue homogenates, resulting in eight calibration standards in each tissue matrix. Low-, medium- and high-concentration QC samples were prepared using a similar preparation method in each matrix. All QC samples were stored at −80 ℃ until analysis.

Preparation of samples The frozen tissue samples were weighed and homogenized in ice cold saline solution (1∶4). The IS solution (10 μL, 5 mg·L^{-1} in methanol) was added to 100 μL of tissue homogenate. Proteins were precipitated by adding acetone (4 ℃, 3 volume) and removed by centrifugation at $10^4\times g$ for 10 min. Residual acetone in supernatants was evaporated under a stream of N_2. Methanol and chloroform (2∶1, *v/v*) were added to the remaining supernatant for liquid-liquid extraction of lipids, which were vortexed for 10 s, and then centrifuged to separate the two phases. The chloroform phases were recovered, evaporated to dryness under N_2, reconstituted in 100 μL methanol before being injected into the HPLC system[13].

Method validation

Selectivity The selectivity of the assay was evaluated, using six lots of different blank matrix, of zero samples (blank matrix added with the IS only), of LLOQ samples, and of samples after single intragastric administration.

Linearity Calibration curves were constructed with the ratios of the peak area of OPA to that of the IS against the theoretical concentrations of OPA in standard samples. Results were fitted to linear regression analysis using 1 / x as a weighting factor.

Accuracy and precision Intra-day precision and accuracy were estimated by analyzing six replicates at three levels of concentration (LQC, MQC and HQC) in a single run. Inter-day precision and accuracy were determined by analyzing the QC samples on three separate days. The accuracy was determined by calculating the difference between calculated and theoretical concentrations. The precision was estimated by the relative standard deviation at each concentration level.

Matrix effect and recovery The absolute/relative matrix effect and recoveries of OPA and the IS were assessed by analyzing three sets of standard samples with three concentrations in six different rats. The absolute matrix effect was evaluated by comparing the mean peak areas of post-extraction blank tissue homogenates that were spiked with standard solutions of OPA and IS (Set 2) with the mean peak areas of post-extraction saline solution spiked with standard solutions (Set 1). The precision (RSD, %) of the analyte peak areas in Set 2 was considered as the relative matrix effect[14]. Recoveries of OPA and the IS were determined by comparing the mean peak areas of analytes added before extraction into the same six different sources as Set 2 (Set 3) with those in Set 2.

Stability In this study, stabilities were constructed with six replicates at two concentration levels (LQC and HQC). The stability of OPA after three cycles of the freeze-thaw processing was evaluated. Further, the post-preparation stability of processed samples at 4 ℃ was assessed to determine whether an occasional delay (3 d) in analysis could lead to instability of the analyte. Short-term stability was determined by allowing QC samples to stand on the bench top for 12 h at room temperature prior to the analysis. Long-term stability of the analyte at −80 ℃ was evaluated by analyzing QC samples over 3 weeks.

Application of the assay Four groups of overnight fasted rats (n = 5 per group) were orally administered OPA at 50 mg·kg^{-1} by gastric intubation which was dissolved in 5% Tween 80 saline solution. This dose was determined by previous studies on pharmacological actions of OPA in mouse. All rats were sacrificed by decapitation at 15, 90, 240, and 600 min post-dosing, separately and the assay was used to calculate concentrations of OPA in different tissue samples at the four time-points (15, 90, 240, and 600 min post-dosing).

Results

1 Chromatography

The product ion mass spectra of OPA and undecylenoylethanolamide are shown in Figure 1. Preliminary studies indicated that the transition conditions of m/z 340.3 → 76.1 for OPA and m/z 228.2 → 62.1 for the IS obtained good specificity and sensitivity for detection and quantification. The collision energy and other optimized parameters used for analytes are presented in Table 1.

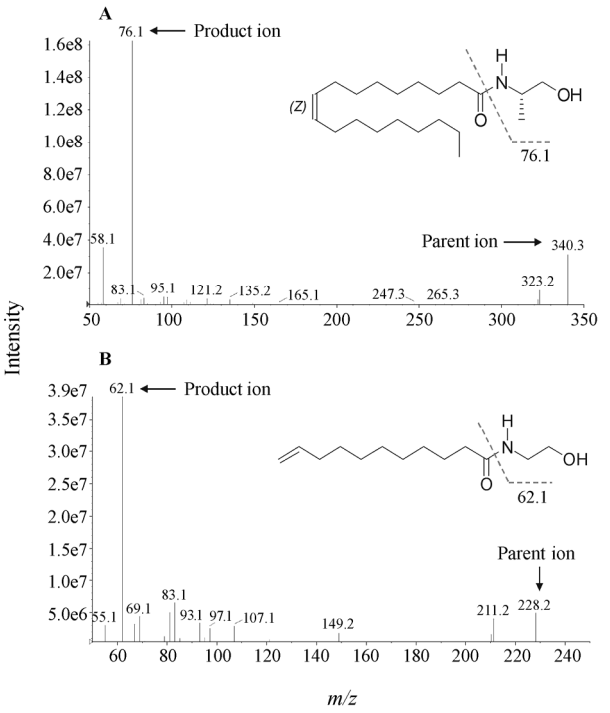

Figure 1 Profile mass spectral data of (A) OPA and (B) undecylenoylethanolamide

Table 1 Tandem mass spectrometric parameters of OPA and the IS. CE: Collision energy; DP: Declustering potential; EP: Entrance potential; CXP: Collision cell exit potential

Compound	OPA	IS
M_r	339.6	227.3
Parent ion	340.3	228.0
Product ion	76.1	62.1
CE /V	35	23
DP /V	55	48
EP /V	5.0	3.5
CXP /V	2.0	2.0
Dwell time /ms	200	200

The chromatographic conditions with retention time of 3.1 min for the IS and 5.1 min for OPA were found to be adequate with apparently symmetric peak for both analytes. The retention time was short and suitable for high-throughput sample determination in pharmacokinetic studies. The ratio of peak area between OPA and IS were optimized in order to reach a sufficient accuracy.

2 Method validation

2.1 Specificity OPA and the IS chromatograms of different blank matrices from six rats indicated that the analyte peaks were well separated from interfering peaks with LLOQ of 1 μg·L^{-1}. Representative chromatograms of OPA in rat liver samples with IS, post-administration plasma and liver samples are shown in Figure 2.

2.2 Linearity The calibration curves for OPA in different tissues appeared to be linear over the concentration ranges tested with the correlation coefficient in excess of 0.999 for all matrices. Table 2 shows the results of a statistical analysis obtained from three runs of calibration curve for OPA.

Table 2 Calibration curves for OPA in rat tissue homogenates (n = 3). y: Peak area ratios of OPA to IS; r: Correlation coefficient

Tissue homogenate	Equation	r	Range /μg·L^{-1}
Brain	$y = 0.002\,87x + 0.005\,42$	0.999 3	5−200
Heart	$y = 0.002\,80x + 0.003\,42$	0.999 5	20−1000
Lung	$y = 0.002\,78x + 0.005\,06$	0.999 7	20−500
Liver	$y = 0.002\,23x + 0.019\,4$	0.999 6	50−500
Spleen	$y = 0.002\,98x + 0.003\,02$	0.999 0	5−200
Kidney	$y = 0.002\,56x + 0.000\,854$	0.999 9	5−500
Small intestine	$y = 0.002\,45x - 0.000\,654$	0.999 6	50−2×10^4
Fat	$y = 0.002\,80x + 0.021\,7$	0.999 1	20−500
Muscle	$y = 0.002\,69x + 0.001\,37$	0.999 8	20−200

2.3 Accuracy and precision Intra-day accuracy (RE) ranged from 96.9% to 107.7% with a precision (RSD) between 1.5% and 10.4%. In addition, the inter-day RE ranged from 96.0% to 107.8% with a RSD between 0.9% and 5.5%. The data showed in Table 3 are average accuracy or precision of the three concentration levels in different tissue homogenates.

2.4 Matrix effect and recovery The data showed in Table 4 are average matrix effect and recovery of LQC, MQC and HQC in tissue homogenates. The absolute matrix effect was ranged from 83.4% and 122.0%,

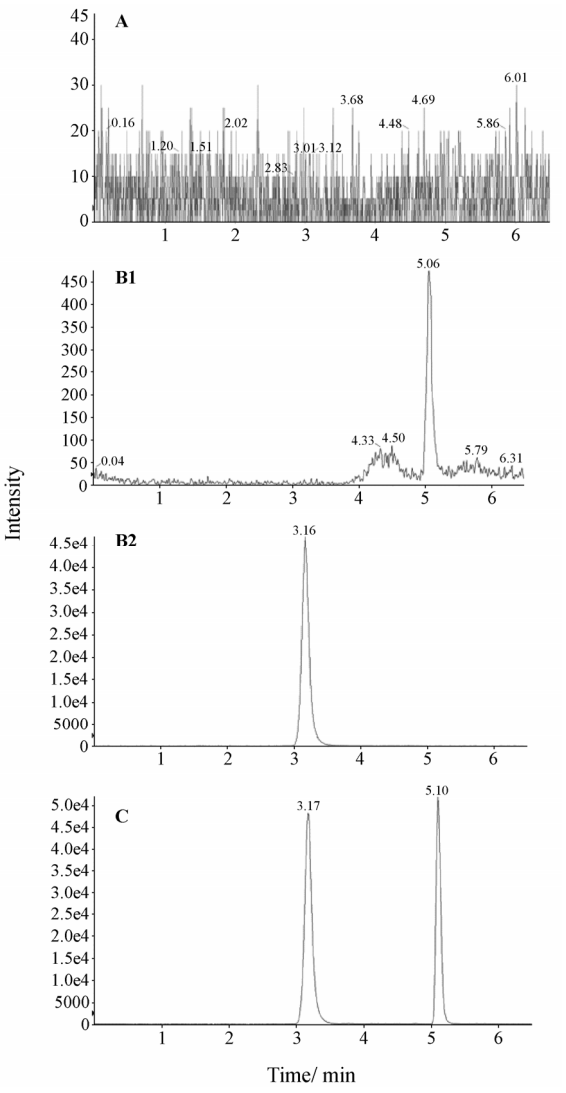

Figure 2 Representative chromatograms of OPA and the IS obtained by extraction of (A) blank rat liver homogenate, (B) liver homogenate spiked with OPA (1 μg·L^{-1}, LLOQ, B1) and the IS (500 μg·L^{-1}, B2), and (C) liver homogenate obtained 15 min after intragastric administration of OPA (50 mg·kg^{-1}) to rats

Table 3 Average accuracy and precision of LQC, MQC and HQC in different tissue homogenates of rats (n = 6). [a]Measured concentration/spiked concentration×100%

Tissue homogenate	Intra-day/%		Inter-day/%	
	Accuracy[a]	RSD	Accuracy[a]	RSD
Brain	101.2	6.3	100.5	1.7
Heart	99.9	2.8	100.0	4.5
Lung	99. 7	2.5	100.0	1.5
Liver	99.6	4.6	100.0	1.9
Spleen	100.8	2.1	100.0	1.8
Kidney	99.9	3.5	100.2	1.7
Small intestine	101.2	4.0	100.0	2.8
Fat	99.6	5.8	101.9	2.4
Muscle	102.4	6.4	101.4	2.6

91.3% and 132.0% for OPA and the IS, respectively. The precision of the peak areas in Set 2 ranged from 1.1% to 7.9% and 1.3% to 7.0% for OPA and the IS, respectively, was considered as the relative matrix effect. The overall recovery of all tissue homogenates was above 70%. The mean recovery for the IS was found to be over 80%. Collectively, these observations indicate that the current sample processing conditions support adequate recoveries for both the analyte and the IS.

2.5 Stability Each stability test included three replicates of two levels of QC samples (LQC and HQC). The results (average levels) are shown in Table 5. No significant changes in OPA concentrations were measured after freeze-thaw processing, or post-preparative at 4 ℃ for 3 d. Long-term and short-term storage had no effect on the stability of OPA as the estimated concentration was close to the theoretical values.

3 Applicability of the assay

Tissue distribution of OPA was investigated following a single oral dose of 50 mg·kg^{-1} to rats. Figure 3 showed that 15 min after administration, most of analyzed tissues contained a significant amount of OPA. The result indicated that OPA underwent a rapid and wide distribution in tissues and organs through the whole body within the time course examined. The highest concentration found in small intestine may be attributed to the residual drug content. Besides small intestine, the highest concentration was found in heart of the nine tissues. The high level concentration in adipose tissue indicated that OPA was possibly stored in this tissue attributed to the structure of long-chain fatty acid, and there was a considerable amount of OPA in brain as well. In terms of clearance, the liver

Table 5 Short-term and long-term stability data of different tissue homogenates (n = 6). A: Bench top stability at room temperature; B: Post-preparative stability at 4 ℃ for 3 d; C: Freeze-thaw stability (3 cycles); D: Long-term stability for 3 weeks (−80 ℃)

Tissue homogenate	Storage condition /%			
	A	B	C	D
Brain	100	101.9	98.9	100.8
Heart	99.9	107.2	101.7	100.6
Lung	99.9	102.7	99.5	103.2
Liver	99.9	102.0	98.9	99.8
Spleen	100.2	102.3	105.4	101.3
Kidney	100.0	100.8	106.4	98.5
Small intestine	100	100.1	100.4	100.2
Fat	100.4	99.3	100.2	100.0
Muscle	100.0	99.8	101.5	105.2

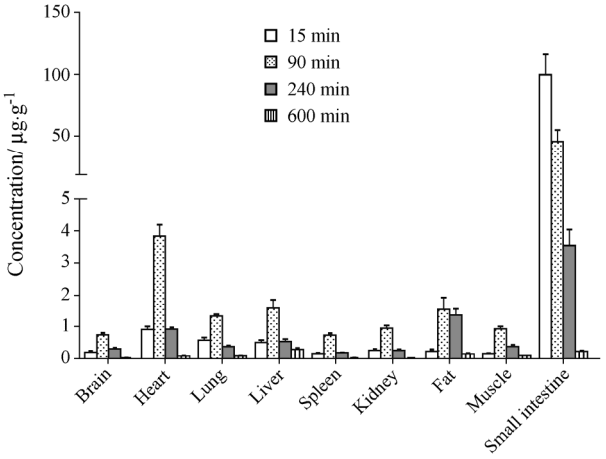

Figure 3 Concentrations (μg·g^{-1}) of OPA in rat tissues at 15, 90, 240, and 600 min after oral administration of OPA at 50 mg·kg^{-1}. n = 5, $\bar{x} \pm s$

Table 4 Matrix effect and recovery evaluation of OPA and the IS in different tissue homogenates (n = 6). [a] Expressed as the ratio of the mean peak area of post-extraction blank matrix that was spiked with standard solutions of an analyte (Set 2) to the mean peak area of post-extraction saline solution spiked with the same standard solutions as Set 2 (Set 1) multiplied by 100. [b] Calculated as the ratio of the mean peak area of an analyte added before extraction to the mean peak area of Set 2 multiplied by 100. [c] Precision of an analyte peak area in Set 2 as the measure of relative matrix effect

Tissue homogenate	Matrix effect[a] /%		Recovery[b] /%		Precision[c] / %		
	OPA	IS	OPA	IS	OPA	IS	OPA/IS
Brain	105.3	107.7	88.0	88.8	2.5	3.3	3.9
Heart	107.7	123.0	79.3	75.9	5.5	4.5	6.6
Lung	90.7	117.0	80.1	73.8	4.1	5.3	6.9
Liver	87.8	101.8	86.9	86.4	4.9	3.5	5.2
Spleen	94.3	108.3	89.1	87.1	4.8	4.1	5.7
Kidney	94.1	109.0	78.3	74.7	3.3	2.3	3.8
Small intestine	109.3	100.1	89.3	73.5	3.0	2.8	2.8
Fat	106.3	101.7	91.4	81.9	2.8	2.4	3.9
Muscle	117.0	106.0	76.8	81.2	4.9	2.8	4.9

initially absorbed much more OPA than the kidneys did.

Discussion and conclusion

For the first time, a highly sensitive and specific method using HPLC-MS/MS for the determination of OPA in different tissue samples (brain, heart, lung, liver, spleen, small intestine, kidney, fat and muscle) of rats was developed and validated. It requires only simple pre-treatment of samples with a chemically related compound, undecylenoylethanolamide, as the internal standard and simplifies the isotope-processing. Differences in analytes' ionization efficiency or sensitivity between the assay reported in this paper and previous studies in quantification of endocannabinoids are due to chromatographic elution and the use of a different IS. But the gradient elution induced a comparatively high matrix effect, especially in low-concentration samples.

The results showed that the highest tissue concentration was observed in small intestine and the level is high in heart. Koga's study has shown that the highest concentration of OEA in peripheral regions was in heart and thymus in 6-week-old rats, and OEA existed in brain with high concentration[15].

The present method should be useful for further studies on anti-hyperlipidemic properties and possible anti-atherogenic properties of OPA by determining the target tissues or organs and evaluating the dose-effect relationship.

References

[1] Desvergne B, Wahli W. Peroxisome proliferator-activated receptor: nuclear control of metabolism [J]. Endocrine Rev, 1999, 20: 649−688.

[2] Staels B, Auwerx J. Role of PPAR in the pharmacological regulation of lipoprotein metabolism by fibrates and thiazolidinediones [J]. Curr Pharm Des, 1997, 3: 1−14.

[3] Fu J, Gaetani S, Oveisi F, et al. Oleylethanolamide regulates feeding and body weight through activation of the nuclear receptor PPAR-α [J]. Nature, 2003, 425: 90−93.

[4] Fu J, Oveisi F, Gaetani S, et al. Oleoylethanolamide, an endogenous PPAR-alpha agonist, lowers body weight and hyperlipidemia in obese rats [J]. Neuropharmacology, 2005, 48: 1147−1153.

[5] Fu J, Astraita G, Gaetani S, et al. Food intake regulates oleoylethanolamide formation and degradation in the proximal small intestine [J]. Biol Chem, 2007, 282: 1518−1528.

[6] Schmid PC, Zuzarte-Augustin ML, Schmid HH. Properties of rat liver *N*-acylethanolamine amidohydrolase [J]. Biol Chem, 1985, 260: 14145−14149.

[7] Cravatt BF, Giang DK, Mayfield SP, et al. Molecular characterization of an enzyme that degrades neuromodulatory fatty-acid amides [J]. Nature, 1996, 384: 83−87.

[8] Lo Verme L, Fu J, Astarita G, et al. The nuclear receptor peroxisome proliferator-activated receptor-α mediates the anti-inflammatory actions of palmitoylethanolamide [J]. Mol Pharmacol, 2005, 67: 15−19.

[9] Chen CX, Zhang HK, Jin X, et al. The effect of *s*-oleylpropanolamide on the expression of cell adhesion molecules in human umbilical vein endothelial cells [J]. Chin J Biochem Pharm (中国生化药物杂志), 2009, 30: 99−102.

[10] Giuffrida A, Piomelli D. Isotope dilution GC/MS determination of anandamide and other fatty acylethanolamides in rat blood plasma [J]. FEBS Lett, 1998, 422: 373−376.

[11] Gonzalez S, Cascio MG, Fernandez-Ruiz J, et al. Changes in endocannabinoid contents in the brain of rats chronically exposed to nicotine, ethanol or cocaine [J]. Brain Res, 2002, 954: 73−81.

[12] Sun CL, Qin W, Zheng JF, et al. Synthesis of oleoylethanolamide analogues [J]. J Xiamen Univ (Nat Sci) (厦门大学学报 自然科学版), 2007, 46: 808−812.

[13] Williams J, Wood J, Pandarinathan L, et al. Quantitative method for the profiling of the endocannabinoid metabolome by LC-atmospheric pressure chemical ionization-MS [J]. Anal Chem, 2007, 79: 5582−5593.

[14] Matuszewski BK, Constanzer ML, Chavez-ENG CM. Strategies for the assessment of matrix effect in quantitative bioanalytical methods based on HPLC-MS/MS [J]. Anal Chem, 2003, 75: 3019−3030.

[15] Koga D, Santa T, Santa T, et al. Liquid chromatographic-atmospheric pressure chemical ionization mass spectrometric determination of anandamide and its analogs in rat brain and peripheral tissues [J]. J Chromatogr B, 1997, 690: 7−13.